Available online at www.sciencedirect.com
ScienceDirect
Molecular & Biochemical Parasitology 154 (2007) 158–169
MOLECULAR & BIOCHEMICAL PARASITOLOGY

Targeted depletion of a mitochondrial nucleotidyltransferase suggests the presence of multiple enzymes that polymerize mRNA 3′ tails in *Trypanosoma brucei* mitochondria

Chia-Ying Kao [1], Laurie K. Read *

Department of Microbiology and Immunology and Witebsky Center for Microbial Pathogenesis and Immunology, SUNY Buffalo School of Medicine, Buffalo, NY 14214, United States

Received 22 January 2007; received in revised form 10 April 2007; accepted 22 April 2007
Available online 27 April 2007

Abstract

Polyadenylation plays an important role in regulating RNA stability in *Trypanosoma brucei* mitochondria. To date, little is known about the enzymes responsible for the addition of mRNA 3′ tails in this system. In this study, we characterize a trypanosome homolog of the human mitochondrial poly(A) polymerase, which we term kPAP2. kPAP2 is mitochondrially localized and expressed in both bloodstream and procyclic form trypanosomes. Targeted gene depletion using RNAi showed that kPAP2 is not required for *T. brucei* growth in either bloodstream or procyclic life stages, nor is it essential for differentiation from bloodstream to procyclic form. We also demonstrate that steady state abundance of several mitochondrial RNAs was largely unaffected upon kPAP2 down-regulation. Interestingly, mRNA 3′ tail analysis of several mRNAs from both life cycle stages in uninduced kPAP2 RNAi cells demonstrated that tail length and uridine content are both regulated in a transcript-specific manner. mRNA-specific tail lengths were maintained upon kPAP2 depletion. However, the percentage of uridine residues in 3′ tails was increased, and conversely the percentage of adenosine residues was decreased, in a distinct subset of mRNAs when kPAP2 levels were down-regulated. Thus, kPAP2 apparently contributes to the incorporation of adenosine residues in 3′ tails of some, but not all, mitochondrial mRNAs. Together, these data suggest that multiple nucleotidyltransferases act on mitochondrial mRNA 3′ ends, and that these enzymes are somewhat redundant and subject to complex regulation.

Keywords: Polyadenylation; RNA stability; Poly(A) polymerase; Trypanosome; Mitochondria

1. Introduction

Polyadenylation of mRNAs is an important posttranscriptional modification that is common to bacteria, as well as the nucleus, cytoplasm, chloroplasts and mitochondria of eukaryotes. Poly(A) tails regulate many aspects of RNA metabolism, including mRNA export, translation, and RNA stability [1,2]. Polyadenylation has very different effects on RNA stability in different systems. For example, in eukaryotic cytoplasm, the poly(A) tail in conjunction with poly(A)-binding proteins increases the stability of many mRNAs [2–5]. On the contrary, in bacteria and chloroplasts, poly(A) tails act as mRNA destabilizing elements [6–8]. In mitochondria from different organisms, polyadenylation exerts different effects on RNA stability. In plant mitochondria, similar to bacteria and chloroplasts, polyadenylation promotes mRNA degradation [9]. Yeast mitochondrial mRNAs lack poly(A) tails. Instead, an encoded dodecamer sequence regulates RNA stability in this system [10]. In human mitochondria, it appears that polyadenylation positively or negatively regulates steady-state levels of mitochondrial mRNAs in a transcript-specific manner [11–13].

The scenario in *Trypanosoma brucei* mitochondria is even more complicated. The synthesis of short (∼20 nt) and long

Abbreviations: PAP, poly(A) polymerase; kPAP2, kinetoplast PAP2; cRT-PCR, circular RT-PCR; CO, cytochrome oxidase; ND, NADH dehydrogenase; CYb, apocytochrome *b*; A6, ATPase subunit 6; RPS12, ribosomal subunit 12; EtBr, ethidium bromide; tet, tetracycline

* Corresponding author at: Department of Microbiology and Immunology, 138 Farber Hall, Buffalo, NY 14214, United States. Tel.: +1 716 829 3307; fax: +1 716 829 2158.
E-mail address: lread@acsu.buffalo.edu (L.K. Read).
[1] Current address: Aaron Diamond AIDS Research Center, The Rockefeller University, 455 First Avenue, New York, NY 10010, United States.

0166-6851/$ – see front matter © 2007 Elsevier B.V. All rights reserved.
doi:10.1016/j.molbiopara.2007.04.014

(∼120–200 nt) mRNA poly(A) tails is developmentally regulated in a transcript-specific manner and coordinated with mRNA editing status [14–18]. Moreover, polyadenylation plays a dual role in modulating RNA stability. In *in vitro* RNA turnover assays, the presence of a poly(A)$_{20}$ tail destabilizes unedited RNAs; however, the same modification stabilizes their partially and fully edited counterparts [19,20]. *In vivo*, the 3′ poly(A) tracts on *T. brucei* mitochondrial RNAs often contain interspersed uridine residues, the distribution of which appears relatively random [18,21–23]. The functional impact of 3′ tracts with differential adenosine/uridine ratios is not well understood. In *in vitro* decay assays, replacement of four adenosine residues within a 20 nt 3′ tail with a stretch of four uridines did not affect the ability of the 3′ tail to stabilize edited RNA [20]. However, the same replacement partially impeded the rapid decay of polyadenylated unedited RNA [19].

To understand how polyadenylation regulates mRNA stability *in vivo*, it is important to identify protein factors that are involved in these pathways, such as poly(A) polymerases (PAPs). Several enzymes have been described to catalyze polyadenylation reactions. The canonical PAP, represented by bacterial class II [24] or eukaryotic class I [25] PAPs, mainly synthesizes homopolymeric adenosine tails. Another enzyme, polynucleotide phosphorylase, which is primarily a degradative enzyme *in vivo*, has been shown to possess polyadenylation activity and create heteropolymeric tails in prokaryotes, cyanobacteria, and chloroplasts of higher plants [26–28]. Recently, a new class of PAPs was described in several eukaryotes. Members of this class include Cid1p and Cid13p in the fission yeast *Schizosaccharomyces pombe* [29,30], GLD-2 in *Caenorhabditis elegans* [31], and hmtPAP in human mitochondria [11,12]. Members of this novel PAP family diverge from canonical PAPs, exhibiting relatively low homology within the catalytic domain. In addition, they lack the C-terminal RNA-recognition motif, which is characteristic for canonical PAPs and is thought to be critical for substrate binding. Therefore, in order for members of this novel PAP family to execute their function, the existence of an associated RNA-binding protein as part of its functional moiety can be postulated. Indeed, Wang et al. have reported that in *C. elegans*, an RNA-binding protein termed GLD-3 binds to and stimulates the polyadenylation activity of GLD-2 [31]. Another member of the novel PAP family, hmtPAP, has been shown to be the *bona fide* mitochondrial PAP in humans [11,12]. Mitochondria from cells in which hmtPAP expression was down-regulated by RNA interference (RNAi) showed decreased poly(A) tail lengths. These alterations in poly(A) tail length exerted positive or negative effects on the steady-state levels of mitochondrial mRNAs in a transcript-specific manner.

As stated above, *in vitro* studies suggest that polyadenylation plays a central role in regulating RNA stability in *T. brucei* mitochondria. Here, we set out to identify mitochondrial PAPs in this system. To this end, we searched for homologs of known mitochondrial PAPs in the *T. brucei* genomic database. A hypothetical protein that was previously designated TbTUT6 [32], which is yet uncharacterized, was found to share the highest sequence homology to the recently identified hmtPAP. Based on the homology of TbTUT6 with hmtPAP and its *in vivo* characteristics described here, we now refer to this enzyme as kinetoplast PAP2 (kPAP2). kPAP2 was initially reported as one of the five putative terminal uridylyltransferases (TUTases) in *T. brucei* based on the sequence similarity of these enzymes to two formerly characterized kinetoplastid RNA editing TUTases, KRET1 and KRET2 [32]. Indeed, TUTases and the novel class of PAPs are similar to each other within their catalytic motif, the nucleotidyltransferase domain. Both types of enzyme belong to the superfamily of nucleotidyltransferase II, which is exemplified by eukaryotic DNA polymerase β [33,34]. Members of this group catalyze template-independent transfer of nucleotides onto the 3′ end of a nucleic acid chain. However, the nucleotide and substrate RNA specificity, processivity, and *in vivo* function of these enzymes cannot be distinguished based on amino acid sequence and need to be determined empirically. Therefore, in this study, we investigated the potential role of kPAP2 in polyadenylation and RNA stability in *T. brucei* mitochondria. We found that kPAP2 is mitochondrially localized and expressed in both bloodstream and procyclic form trypanosomes. Targeted gene depletion using RNAi showed that kPAP2 is not required for *T. brucei* growth in either bloodstream or procyclic life stages, nor is it essential for differentiation from bloodstream to procyclic form. The steady state abundance of several mitochondrial RNAs was also largely unaffected upon kPAP2 down-regulation. Interestingly, when we sequenced the 3′ tails of several mRNAs, we found that different mRNAs possess 3′ tails of very specific length and uridine content. Upon kPAP2 depletion, mRNA-specific tail lengths were maintained. However, the percentage of uridine residues in 3′ tails was increased, and the percentage of adenosine residues correspondingly decreased, upon kPAP2 down-regulation in a distinct subset of mRNAs. Thus, kPAP2 apparently contributes to adenosine incorporation into mRNA 3′ ends in some, but not all, mitochondrial mRNAs. In sum, these results suggest that multiple nucleotidyltransferases act on mRNA 3′ ends, and that these enzymes are somewhat redundant and regulated in a transcript-specific manner.

2. Materials and methods

2.1. Oligonucleotides used in this study

The oligonucleotides used in this study are listed as follows with restriction sites or T7 promoter sequence (for CR6-5′T7) underlined: RXS-dT$_{17}$ (5′ GAGAATTCTCGAGTCGACTTTTTTTTTTTTTTT 3′); mtPAP-5′-EXP (5′ CCCAAGCTTATGGCTTTAGTTCGTAGGATAGG 3′); mtPAP-3′-EXP (5′ GCTCTAGACTCGAGAACACTAGAAAGCCTTCCTTGTTT 3′); mtPAP5′i (5′ GCGGATCCATGCTGATTACGCAGTGTTATTT 3′); mtPAP3′i (5′ CCATCGATCTTAAAACATTCTGTATGTCAACGT 3′); Tub-RT (5′ GGGGGTCGCACTTTGTC 3′); Tub-5′ (5′ GGACTATGGCAAGAAGTCC 3′);12S-1 (5′ GCTTGTTAACCTGCTCGAAC 3′); CYb-D (5′ CCTGACATTAAAAGACCCTTTCTTTTTTCTC 3′) CYb-R (5′ CCTGACATTAAAAGACAACACAAATTTCTAAA 3′) CR6-5′T7 (5′ TGTAATACGACTCACTATAGGGCTAATACACTTTTGATAACAAACTAAAGTAAA 3′); CR6-3′E (5′ AAAAACATA-

TCTTATATCTAAATCTAACTTACAATACGT 3′); COI-RT (5′ GTAATGAGTACGTTGTAAAACTG 3′); ND1-RT2 (5′ AAAGCAATTTTGTAAAGAAAGTTG 3′) ND4-RT (5′ GATAAAAATATTAGTGACATTG 3′); CO2-RT (5′ ATTTCATTACACCTACCAGG 3′); CYb-RT (5′ CAACCTGACATTAA AAGAC 3′); A6-3′NE (5′ GCGGATCCATTTGATCTTATTCTATAACTCC 3′); ND7-5′-RT (5′ CACATAACTTTTCTGTACCACGATGC 3′); CO3-3′NE (5′ ACTTCCTACAAACTAC 3′) COI-RT (5′ GTAATGAGTACGTTGTAAAACTG 3′) COI-1 (5′ CCAATCATTTTATGAGAAACACTTAAGCACACAAGACATAG 5′) COI-lower (5′ CGTATTTTATATTTTTTTTTGACAAG 3′) RPS12-2b (5′ GC GGATCCTTATTCAAAAGAAGCTCTCCGTCG 3′) CR6-5′NE (5′ ACTTTAGTTTGTTATCAAAAGTGTATTAG 3′) CR6-3′U (5′ CATCGTTTAGAAGAGATTTTAGAA 3′) CYb-cRT1 (5′ AAATCCTAAACTAAAACCTACCC 3′) CYb-cRT2 (5′ TATGAATGGAATTACAATACTGAG 3′) 12S-2 (5′ CGGGATCCATTAAAAATAAATGTGTTTCATCGTC 3′) 12S-3 (5′ CATTATTATAATATTCTTCTTAATTGG 3′).

2.2. cDNA cloning and plasmid construction

A BLAST search of the *T. brucei* genomic database (Wellcome Trust Sanger Centre and the Institute for Genomic Research *T. brucei* databases) revealed a hypothetical protein (Tb10.100.0050; hereafter referred to as kPAP2) that shares homology to human mitochondrial PAP. To clone kPAP2, total procyclic form cDNA was generated by reverse transcription primed with [dT]-RXS. The entire kPAP2 ORF was amplified using oligonucleotides mtPAP-5′-EXP and mtPAP-3′-EXP, which were designed based on the genomic sequence. To construct tetracycline (tet) regulatable Myc100-kPAP2 plasmid, the aforementioned PCR product was digested with XbaI and HindIII, and then ligated into the same sites of Myc100 vector [35]. The resulting plasmid encodes a tet-regulated full-length kPAP2 gene fused with two copies of myc epitope at the C-terminus.

2.3. Trypanosome culture, mitochondrial isolation, transfection, induction of RNAi, and differentiation

Procyclic form *T. brucei brucei* clone IsTaR1 stock EATRO 164 was grown as described by Brun and Schonenberger [36]. The bloodstream form *T. brucei brucei* 221a variant (MiTat 1.2a), which expresses the *VSG 221* from the *221* ES, was maintained as described [37]. Mitochondria were isolated according the method of Harris et al. [38]. Procyclic *T. brucei brucei* strain 29-13, which contains integrated genes for T7 RNA polymerase (T7RNAP) and tetracycline repressor (TetR), were grown in SDM-79 medium supplemented with 15% fetal bovine serum (FBS) at 27 °C as described previously [36,39] in the presence of G418 (15 μg/ml) and hygromycin (50 μg/ml). The bloodstream single-marker cell line, which also expresses T7RNAP and TetR, were maintained in HMI-9 medium supplemented with 10% FBS and 10% Serum Plus (JRH Biosciences) at 37 °C/5% CO_2 as described previously [37] in the presence of G418 (2.5 μg/ml). Bloodstream form 221a cells, single marker cells, and procyclic form 29-13 cells were all generously provided by Dr. George Cross.

To construct the p2T7-177-kPAP2 vector for RNAi, a 476 bp fragment of the kPAP2 gene (nucleotides [nt] 200–675 from the start codon) was amplified by PCR with oligonucleotides mtPAP5′i and mtPAP3′i. The fragment was digested and inserted into the BamHI/ClaI sites of p2T7-177 vector [40]. For procyclic transfection, 1×10^9 cells were washed once in 100 ml of ice-cold EM buffer [41] and resuspended in fresh EM buffer to a concentration of 2.5×10^7 cells/ml. One hundred micrograms of p2T7-177-kPAP2 plasmid linearized with NotI was then added to 0.45 ml of cells. Transfections were carried out on ice in 2 mm cuvettes using a Bio-Rad electroporator with two pulses at the following settings: 800 V, 25 μF, and 40 Ω. Following electroporation, 0.25 ml of the cell suspension was transferred into 4 ml SDM-79 (15% FBS) in the presence of G418 and hygromycin and allowed to recuperate for 20 h. Selection was then applied by the addition of 2.5 μg/ml phleomycin, and the cells were grown for 3 weeks to obtain stable transfectants. For bloodstream transfection, 5×10^7 cells were washed in 50 ml ice-cold EM buffer [41] and resuspended in fresh EM buffer to a concentration of 2.5×10^7 cells/ml. One hundred micrograms of p2T7-mtPAPi plasmid linearized with NotI was added to 0.6 ml of cells. Electroporations were performed on ice in 4 mm cuvettes using a Bio-Rad electroporator with one pulse at the following setting: 1990 V, 25 μF, and 25 Ω. Following electroporation, the entire 0.6 ml of cell suspension was transferred into 50 ml HMI-9 (10% FBS and 10% Serum Plus) in the presence of G418, and allowed to recover for 20 h. Selection was applied by the addition of 2.5 μg/ml phleomycin, and stable transfectants were obtained on day 6 post drug selection. Clonal lines were obtained by serial dilution.

For induction of double-stranded RNA (dsRNA), procyclic or bloodstream transfectants were cultured in the presence of 1 and 2.5 μg/ml tet, respectively. Growth curves were obtained by plotting the total cell number (the product of the cell number and the total dilution) over a period of 10–12 days.

Differentiation of bloodstream form kPAP2 RNAi cells was carried out based on the protocol developed by Brun and Schonenberger [42]. Briefly, bloodstream form cells ($1–2 \times 10^6$ cells/ml) cultured in HMI-9 medium were collected by centrifugation, and then resuspended into Cunningham's media (JRH Biosciences) with 6 mM *cis*-aconitate and 6 mM citric acid at a concentration of 2×10^6 cells/ml, accompanied by a drop in culture temperature from 37 to 27 °C. For kPAP2 RNAi cells, differentiation was initiated on day 4 following tet-induction.

2.4. RNA analysis

Total RNA was purified from 1 to 2×10^9 cells (Purescript RNA isolation kit; Gentra Systems). For PCR analysis, cDNA was synthesized from 10 μg of total RNA by using oligonucleotide RXS-dT_{17}. Ten percent of the resulting cDNA was used as a template for amplification of the full-length kPAP2 ORF (oligonucleotides mtPAP-5′-EXP and mtPAP-3′-EXP) or a 445-

bp fragment of the tubulin cDNA (oligonucleotides Tub-RT and Tub-5′). cDNA was titrated to ensure that PCRs were performed in the linear range. For northern blot analysis, 10–20 μg of total RNA was electrophoresed on 1.5% formaldehyde–agarose gels and transferred to nylon membrane. Blots were probed with kinase-labeled oligonucleotide probes 12S-1 for detection of 12S RNA, CYb-D for unedited CYb RNA, and CYb-R for edited CYb RNA. For northern blot analysis of edited RPS12 mRNA, a radiolabeled DNA probe corresponding to the full-length fully edited RPS12 sequence was generated by PCR reaction using oligonucleotides CR6-5′T7 and CR6-3′E with [α-^{32}P]dATP, and hybridization was performed as described previously [17]. Poisoned primer extensions using oligonucleotides Tub-RT, COI-RT, ND1-RT, ND4-RT, CO2-RT, CYb-RT, A6-3′NE, ND7-RT and COIII-3′NE were performed with 20 μg of total RNA as described previously [43]. Gels were analyzed by phosphoimager analysis on a Bio-Rad Personal FX Phosphoimager using Quantity One software.

For circular RT-PCR (cRT-PCR) analysis, the protocol described by Kuhn and Binder [44] was adopted with slight modification. In short, 10 μg of RNA was circularized with T4 RNA ligase in a total volume of 25 μl, following the instruction of the manufacturer (New England Biolabs). Resulting circular RNA was subjected to standard phenol:chloroform extraction and ethanol precipitation, and then resuspended in 30 μl of distilled water. cDNA was synthesized using the self-ligated RNA, 5 pmol of gene-specific primers (COI: COI-RT; RPS12U: RPS12U-2b; CYb: CYb-cRT1; 12S rRNA: 12S-1), and SuperScript III Reverse Transcriptase (Invitrogen). The first-strand cDNA was subjected to PCR with appropriate primer pairs (COI: COI-1 and COI-lower; RPS12U: CR6-5′NE and CR6-3′U; CYb: CYb-cRT1 and CYb-cRT2; 12S rRNA: 12S-2 and 12S-3) flanking the 3′ and 5′ end joining sites. The PCR products were cloned into pCR2.1-TOPO vector using TOPO TA Cloning kit (Invitrogen). Plasmids with inserts were submitted to sequencing with vector primers (RPCI DNA Sequencing Laboratory).

2.5. Western blot analysis

For analysis of the subcellular localization of myc-kPAP2, 10 or 25 μg of whole cell or mitochondrial extracts from procyclic form trypanosomes expressing myc-kPAP2 were electrophoresed in SDS-PAGE (10% polyacrylamide) and transferred to nitrocellulose membranes. Blots were probed with anti-myc (1:6000 dilution; a generous gift from Dr. Alfred Ponticelli), anti-RBP16 (1:1:000 dilution; [45]), or anti-β tubulin (1:1000; Sigma–Aldrich) primary antibodies. For differentiation studies, aliquots (1×10^6 cells) of uninduced and induced kPAP2 RNAi cells were suspended in SDS-PAGE sample buffer immediately after harvesting, boiled for 5 min, and stored at −80 °C until use. After SDS-PAGE electrophoresis and transfer steps, blots were probed with anti-VSG221 (1:10,000 dilution; a generous gift from Dr. George Cross [46]) and anti-GPEET procyclin (1:2000 dilution; Cedarlane) as primary antibodies. Primary antibodies were detected by incubation with horseradish peroxidase conjugated goat anti-mouse antibodies (1:10,000 dilution; Pierce) for anti-myc and anti-GPEET procyclin antibodies, or horseradish peroxidase conjugated goat anti-rabbit antibodies (1:10,000 dilution; Pierce) for anti-RBP16, anti- β tubulin, and anti-VSG221, and then detected by enhanced chemiluminescence (Pierce).

3. Results

3.1. kPAP2 encodes a homolog of hmtPAP

To identify a homolog of hmtPAP, we performed a BLAST search of the *T. brucei* GeneDB database (Sanger Institute) using hmtPAP as the query. A hypothetical protein previously designated TbTUT6 [32] based on its sequence homology to RNA editing TUTases emerged with the highest matching score (*E*-value: 1.6E−08). The next highest match, TbTUT4, had a score of 2.7E−07. However, TbTUT4 has been recently demonstrated to be a cytoplasmic TUTase [47], and is unlikely to be involved in mitochondrial polyadenylation. No other protein with an *E*-value lower than E−5, which is the typical threshold for highly unique alignments, was identified by the search. Therefore, we focused our study on the previously designated TbTUT6 protein. Based on the high degree of sequence homology between hmtPAP and this protein, in conjunction with *in vivo* data described below, it is hereafter referred to as kinetoplast PAP2 (kPAP2). (Another enzyme, which displays PAP activity *in vitro*, has previously been referred to as kPAP1 (R. Aphasizhev, pers. comm.; Woods Hole Molecular Parasitology Meeting XVII, #217B).)

A search for defined protein motifs in kPAP2 using the InterProScan tool (EBI Server) revealed that this protein contains several conserved domains. Among the most significant with respect to its putative function were the class II nucleotidyltransferase domain (InterPro unintegrated domain no. SSF81301), PAP/25A core domain (InterPro accession no. IPR001201), and PAP/25A-associated domain (InterPro accession no. IPR002058) (Fig. 1). Furthermore, a mitochondrial localization sequence was predicted for this protein by multiple topology prediction programs, including PSORTII, TargetP 1.1, and MITOPROT (Fig. 1B). kPAP2 shares 26% identity and 45% similarity to hmtPAP within a 244 amino acid (aa) conserved domain, which encompasses the nucleotidyltransferase motif and PAP/25A core domain (Fig. 1A). When aligned with hmtPAP, kPAP2 apparently lacks the N-terminal sequence (∼200 amino acid long) immediately upstream of the catalytic domain, which is present in hmtPAP and its orthologs in other mammalian systems (Fig. 1A). The absence or presence of this domain largely accounts for the difference between the sizes of kPAP2 (375 aa) and hmtPAP (582 aa). The sequences downstream of the catalytic motif, which include a portion of the PAP/25A associated domain, are not well conserved between kPAP2 and hmtPAP. As stated above kPAP2 also displays homology to known TUTases. However, multiple alignment of the kPAP2 amino acid sequence with those of RET1, RET2, and TUT3 reveals that kPAP2 lacks the ∼100 nt insertion found in the middle domain of these TUTases (data not shown) [47]. Absence

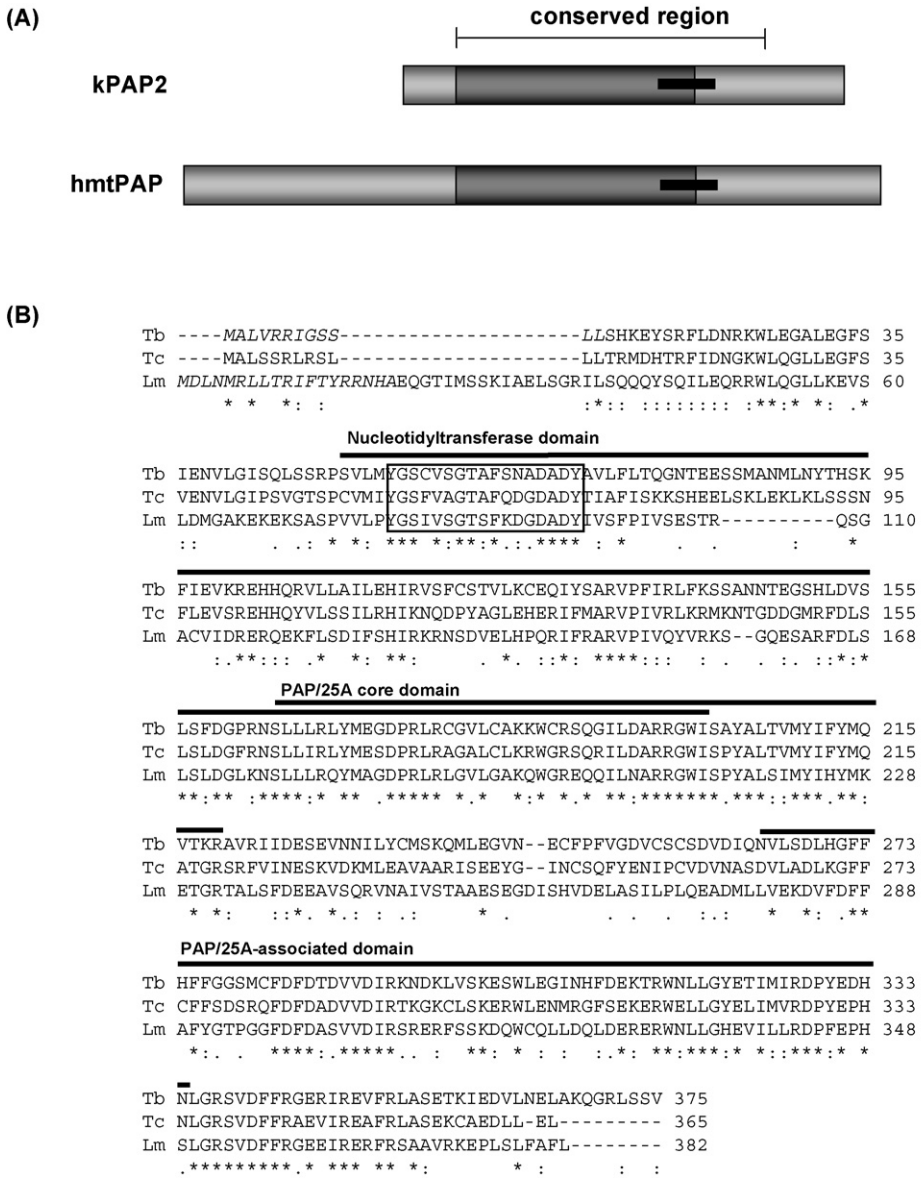

Fig. 1. kPAP2 amino acid sequence analysis. (A) Schematic diagram comparing *T. brucei* kPAP2 and human mitochondrial PAP (hmtPAP, accession no. NP_060579) proteins. Class II nucleotidyltransferase domains are shaded dark grey. PAP/25A core domains, which overlap the nucleotidyltransferase domains, are indicated by a thick, black line. kPAP2 and hmtPAP are 26% identical and 45% similar within the 244 amino acid conserved region. (B) Clustal W alignment of full-length kPAP2 homologs from *T. brucei*, *T. cruzi*, and *L. major*. Conserved domains detected using InterProScan tool (EBI Server) are indicated above each bold line that marks the range of the domain: class II nucleotidyltransferase domain (InterPro unintegrated domain no. SSF81301), PAP/25A core domain (InterPro accession no. IPR001201), and PAP/25A-associated domain (InterPro accession no. IPR002058). The signature sequence of the Pol β superfamily of nucleotidyltransferases (hGS X_{10} DXDh) is boxed [34]. Predicted mitochondrial import sequences are shown in italics. (*) Indicates identical residues, (:) indicates conserved substitutions, and (.) indicates semi-conserved substitutions.

of this TUTase-specific insertion is consistent with a role for kPAP2 in polyadenylation as opposed to uridylation. kPAP2 is conserved among kinetoplastids. In addition to the previously reported ortholog in *Leishmania major* database [32], BLAST search also revealed an apparent ortholog in *T. cruzi* (Fig. 1B). The degree of amino acid identity between full-length *T. brucei* kPAP2 and its orthologs in other kinetoplastids is 55% in *T. cruzi* and 41% in *L. major*. The kPAP2 ortholog in *L. major* also contains a predicted mitochondrial localization sequence. Conservation of kPAP2 suggests that this protein plays an important role in kinetoplastid biology.

3.2. kPAP2 is constitutively expressed and mitochondrially localized

To begin functional analysis of kPAP2, we first examined the mRNA expression profile in both bloodstream and procyclic form parasites. Equal microgram amounts of total RNA from both life stages were isolated, and northern blot analysis was performed using a riboprobe complementary to the full-length kPAP2 coding region (1128 nt). A single band at ∼1300 nt was detected in both life stages at similar intensity (Fig. 2A), suggesting that kPAP2 functions throughout the trypanosome life cycle.

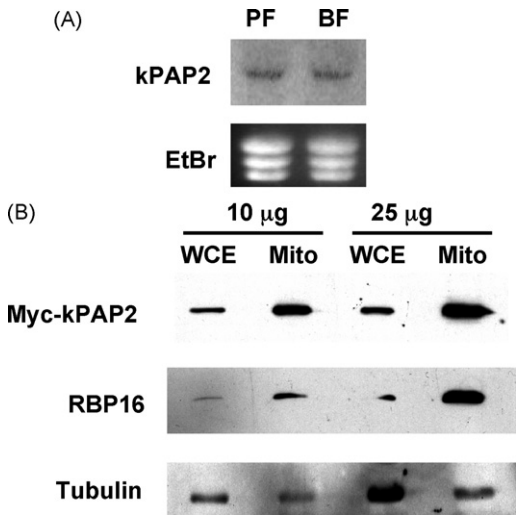

Fig. 2. kPAP2 is constitutively expressed and mitochondrially localized. (A) Twenty micrograms of total RNA isolated from procyclic (PF) and bloodstream (BF) form trypanosomes were subjected to northern blot analysis. kPAP2 mRNA was detected by full-length riboprobe. Ethidium bromide staining of ribosomal RNAs is shown to indicate loading. (B) Anti-myc antibodies were used to probe blots containing 10 or 25 μg of whole cell (WCE) or mitochondrial (mito) extracts prepared from procyclic form *T. brucei* cells that express Myc-kPAP2 protein. RBP16 levels were detected with anti-RBP16 antibodies, and are shown as a positive control for a known mitochondrial protein. Tubulin was detected using anti-tubulin antibodies, and is shown as a control for proteins that are not enriched in mitochondria.

We next sought to verify that kPAP2 is indeed a mitochondrial protein. Due to the lack of antibody against endogenous kPAP2, we created trypanosomes that stably express a tet-inducible C-terminally tagged myc-kPAP2. We were unable to obtain stable clones in procyclic form cells, but did generate bloodstream form cell lines expressing myc-kPAP2. Because procyclic form trypanosomes, unlike their bloodstream form counterparts, contain mitochondria that are both cristae-rich and competent in oxidative phosphorylation, we differentiated the bloodstream from transfectants to procyclic form prior to induction of myc-kPAP2. Differentiation was confirmed by monitoring the expression of stage-specific surface markers, VSG and GPEET-procyclin, by western blot analysis. Three days post induction, whole cell and mitochondrial extracts were prepared from myc-kPAP2 expressing procyclic cells, and equal microgram amounts of extracts were subjected to western blot analysis using anti-myc antibody. A band corresponding to the calculated molecular weight of myc-kPAP2 fusion protein (~42 kDa) was detected in both whole cell and mitochondrial extracts. This protein was enriched approximately 14-fold in mitochondrial lysates (Fig. 2B, upper panel). This degree of enrichment is similar to that observed for a known mitochondrial protein, RBP16, which was probed on the same blot (Fig. 2B, middle panel). Tubulin, which is mainly localized to microtubules and flagella, was relatively depleted in mitochondrial extracts, demonstrating the quality of cell fractionation (Fig. 2B, lower panel). Thus, consistent with its predicted mitochondrial import sequence, kPAP2 is mitochondrially localized in procyclic form *T. brucei*.

3.3. Knockdown of kPAP2 has no effects on survival, growth, or differentiation of T. brucei

To determine the function of kPAP2, we first sought to characterize the enzymatic activity of kPAP2 *in vitro*. kPAP2 generated by *in vitro* transcription/translation was inactive (data not shown). Next, using the myc-tagged kPAP2 cell extracts, we performed pull-down assays with anti-myc antibody under several wash conditions. The affinity-purified myc-kPAP2 was used for *in vitro* nucleotide incorporation assay under several assay conditions with various cationic species and concentrations, as well as different nucleotide triphosphates and RNA substrates, yet no enzymatic activity was detected (data not shown). Thus, we were unable to determine the nucleotide specificity or enzymatic activities of kPAP2 *in vitro*.

We, therefore, turned to *in vivo* studies of kPAP2 function using RNA interference (RNAi) approaches. A 476-bp fragment of the kPAP2 coding region corresponding to nts 200–675 from the start codon was cloned into p2T7-177 vector between opposing T7 promoters [40]. The resulting construct was transfected into either procyclic *T. brucei* 29-13 cells or bloodstream single marker cells, both of which express TetR protein and T7RNAP [39]. Stable clonal cells that had integrated the kPAP2 fragment into the 177 bp repeat locus on the minichromosomes were selected by phleomycin treatment and used for subsequent analyses. RNAi was induced by addition of 1 (procyclic form) or 2.5 (bloodstream form) μg/ml tetracycline, and the knockdown of kPAP2 mRNA in both procyclic and bloodstream form clonal cells was demonstrated by RT-PCR (Fig. 3A) and confirmed in procyclic cells by northern blot analysis (data not shown). Cell growth was monitored in induced versus uninduced procyclic and bloodstream form kPAP2 RNAi cells, and no apparent difference in growth rate or cell morphology was observed in either life stage (Fig. 3A). These results suggest that kPAP2 is not essential for the survival or growth of the parasites. Alternatively, the residual small quantity of kPAP2 present in the knockdown cells is sufficient to carry out the tasks required for maintaining normal cell growth.

Although down-regulation of kPAP2 in both procyclic and bloodstream form parasites failed to show any growth phenotype, generation of bloodstream RNAi cells allowed us to investigate the role of kPAP2 during bloodstream to procyclic form differentiation. *In vitro*, bloodstream form *T. brucei* differentiates readily to procyclic form in response to environmental cues, including temperature shift from 37 to 27 °C, and the presence of ≥3 mM citrate and/or *cis*-aconitate [42]. Differentiation from the bloodstream to procyclic forms can be assessed by the disappearance and appearance of stage-specific surface antigens, as well as by change of cell morphology. To explore the possible role of kPAP2 during differentiation, we tested whether bloodstream form trypanosomes are capable of differentiating to procyclic forms following kPAP2 knockdown. kPAP2 knockdown was induced in bloodstream RNAi cells 4 days prior to differentiation initiation, since down-regulation of kPAP2 expression is apparent on day 4 of tet induction (Fig. 3A, right). Cells were monitored daily by light microscopy during the differentiation process. Prior to differentiation initiation and 2, 4,

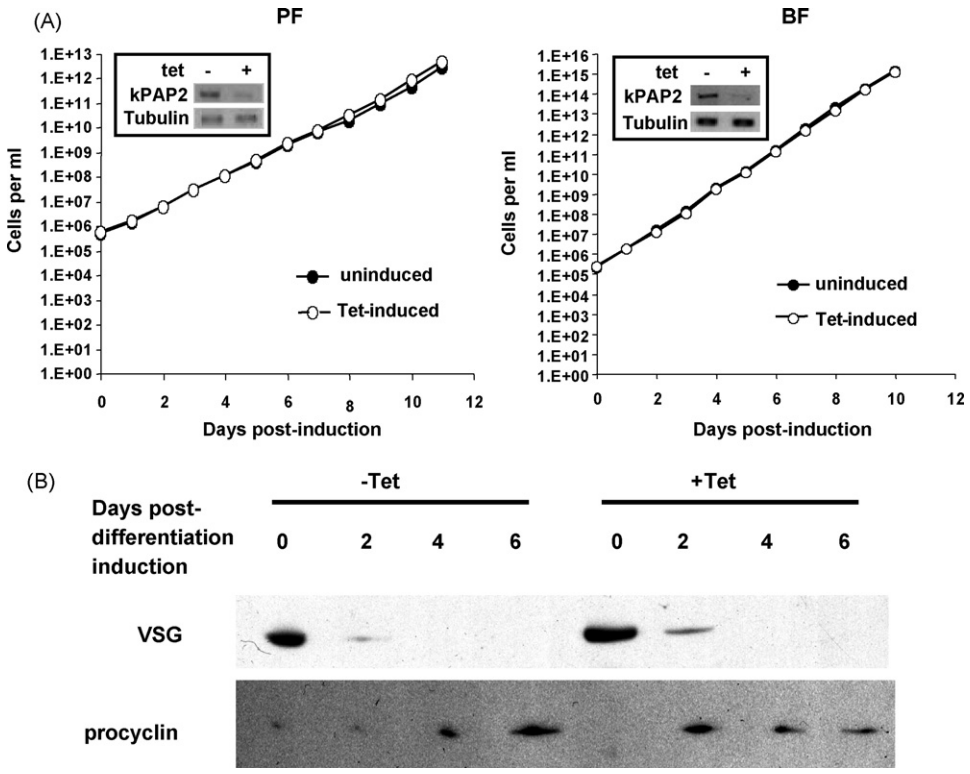

Fig. 3. Knockdown of kPAP2 has no effects on survival, growth, or differentiation of *T. brucei*. (A) Growth of PF (left) and BF (right) *T. brucei* kPAP2 RNAi cells either uninduced (close circles) or induced with 1 μg (PF) or 2.5 μg (BF) of tet (open circles). Growth curves were obtained by plotting the total cell per ml as the product of the cell density and the total dilution. As shown in the insets, kPAP2 mRNA levels were monitored by PCR amplification of full-length kPAP2 RNA in induced and uninduced cells on day 4 after tet addition. Tubulin RNA levels were monitored as a control. (B) Bloodstream form kPAP2 RNAi cells were induced with tet for 4 days, and then induced to differentiate into procyclic forms. Aliquots of 1×10^6 cells of uninduced and tet-induced kPAP2 RNAi cells were analyzed by western blot prior to differentiation initiation, and on days 2, 4, and 6 post-differentiation initiation. Blots were probed with antibodies against VSG221 and GPEET procyclin to monitor differentiation.

and 6 days post-differentiation initiation, samples of whole cell extract equivalent to 1×10^6 cells were prepared and subjected to western blot analyses using anti-VSG and anti-procyclin antibodies (Fig. 3B). A comparable rate of differentiation, depicted by similar kinetics of VSG loss and procyclin appearance, was observed for both uninduced and induced cells. The slight difference on day 2 (Fig. 3B) was not reproducible. From these data, we conclude that that kPAP2 is dispensable for the differentiation of trypanosomes *in vitro*, or that residual amounts of enzyme suffice for this purpose.

3.4. Analysis of 3′ tail length and nt content in procyclic and bloodstream form kPAP2 RNAi cells

Since we speculated that kPAP2 contributes to polyadenylation of mitochondrial RNAs due to its sequence homology to hmtPAP, we examined the effect of kPAP2 knockdown on mRNA 3′ tail length and sequence. Both short (∼20 nts) and long (∼120–200 nts) poly(A) tails are found on the 3′ ends of trypanosome mitochondrial transcripts [16–18,21,49], and the poly(A) tails often contain interspersed uridine residues [18,21–23]. To examine whether kPAP2 depletion has an effect on the length and/or sequence composition of 3′ tails of mitochondrial mRNAs, we employed the circular RT-PCR (cRT-PCR) method [44]. For this analysis we isolated total RNA from uninduced and tet-induced kPAP2 RNAi cells from both bloodstream and procyclic stages. RNA 5′ and 3′ ends were joined by T4 RNA ligase, cDNAs were synthesized using RNA specific primers, and oligonucleotide pairs that amplify the regions encompassing the ligated 5′ and 3′ ends for specific mitochondrial transcripts were used for the PCR reaction. This method may bias toward the analysis of short-tailed RNA, since PCR products derived from long-tailed RNAs are less likely to be amplified and cloned. In this analysis, we examined the 3′ extensions of three different mRNAs that span different degrees of editing and different life cycle stage regulation: cytochrome oxidase I (COI), ribosomal protein S12 (RPS12), and apocytochrome *b* (CYb). COI is a never-edited mRNA, and it was examined in both bloodstream and procyclic life cycle stages. RPS12 is an extensively edited RNA, and both unedited and edited versions of this RNA are upregulated in bloodstream *T. brucei* [17] (see also Fig. 4). Thus, we analyzed RPS12 unedited (RPS12U) RNA 3′ ends in bloodstream parasites. CYb is edited in a small domain at its 5′ end. CYb RNA is exclusively edited in procyclic stage parasites, and it was analyzed in this life cycle stage.

Results of mRNA 3′ tail analyses in uninduced and induced kPAP2 cells are presented in Tables 1 and 2. Tail lengths ranged from 13 to 54 nt in those RNAs examined. Strikingly, in uninduced cells, the average tail length for a given mRNA species

Table 1
mRNA 3′ tail length and nt composition in kPAP2 RNAi cells

	−Tet			+Tet		
RNA[a]	# clones	Tail length	Percent uridine residues	# clones	Tail length	Percent uridine residues
BF COI	10	17 ± 4	3.4 (5/147)	12	21 ± 7	3.9 (9/231)
BF RPS12U	18	38 ± 7	3.3 (23/689)	18	40 ± 9	8.7 (64/736)
PF COI	6	20 ± 4	1.0 (1/102)	5	22 ± 4	2.0 (2/101)
PF CYb[b]	3	47 ± 7	24.1 (34/141)	2	42 ± 0	22.9 (29/83)

[a] BF: RNA isolated from bloodstream form kPAP2 RNAi cells; PF: RNA isolated from procyclic form kPAP2 RNAi cells; COI: cytochrome oxidase subunit I, RPS12U: unedited ribosomal subunit 12; CYb: apocytochrome *b*.
[b] −Tet CYb clones consisted of one unedited and two partially edited; +Tet CYb clones were both partially edited.

was distinct. The longest tails were found on procyclic form CYb RNA (in our analysis, consisting of primarily partially edited RNAs), averaging 47 nt. 3′ tails on bloodstream form RPS12U were just slightly shorter, at an average of 38 nt. In contrast, COI mRNA 3′ tails were consistently much shorter, averaging 17 and 20 nt in bloodstream and procyclic form parasites, respectively. These analyses indicate that 3′ tail lengths are mRNA-specific and, at least for COI mRNA, the lengths of these relatively short tails do not change during life cycle stage differentiation. (As stated above, the ∼120–200 nt tail class is probably excluded from the cRT-PCR analysis.) Upon kPAP2 down-regulation, mRNA-specific tail lengths were largely maintained (Table 1). Thus, we conclude that mitochondrial enzymes other than kPAP2 are capable of synthesizing mRNA 3′ tails.

Table 2
Number of uridine addition sites and sequences of RPS12U 3′ tails in BF kPAP2 RNAi cells

−Tet	+Tet
No U's	
A_{31}	A_{27}
A_{38}	A_{31}
A_{44}	A_{35}
$A_{27}CACA_6$	A_{43}
	A_{44}
One site	
$A_{25}UA_2$	A_4UA_{27}
$A_{21}UA_7$	$A_{28}UA_{12}$
$A_{27}UA_3$	$A_{20}CA_{22}UA_3$
$A_{25}UA_9$	
$A_{20}UA_{12}$	
$A_{17}UA_{25}$	
$A_{40}UA_4$	
$A_{44}U$	
$A_4UA_{10}CA_{31}$	
Two sites	
$A_3UA_{34}UC_2$	$AUA_{37}U$
$A_8UA_{12}UA_{13}$	$A_2U_2A_2U_3A_{20}$
$A_{18}U_2A_4UA_4$	$A_{10}U_4A_{11}UA_{19}$
$A_{43}UA_3U$	$A_{16}UA_{17}UA_2$
	$U_4A_2U_7A_{35}$
	$AU_2A_{36}UA_4$
>Two sites	
$A_{20}U_3A_{11}UA_{11}UA_4$	$AUAU_2A_8U_2A_6GA_{13}$
	$AU_2A_4UA_{13}UA_{16}CA_{10}$
	$U_4A_{20}UA_7UA_2UA_6$
	$U_4A_3U_4A_4UA_4U_2A_3UA_{10}UAUA_3UA_{18}UA_3U$

We also quantified the percent of uridine residues in mRNA 3′ extensions in uninduced and induced kPAP2 cells (Table 1). Again, we were surprised to find a very significant mRNA-specific difference in 3′ tail nt content. In uninduced cells, COI and RPS12U RNA 3′ extensions consisted of between 1% and 3% uridine residues, with the remainder of nucleotides primarily adenosines. CYb mRNA 3′ tails, on the other hand, contained approximately 10-fold higher uridine content, with an average of 24% uridine residues. Thus, the percentage of uridine residues in mRNA 3′ tails is RNA-specific, and it is not correlated with either life cycle stage or overall 3′ tail length. We next asked whether kPAP2 down-regulation affects mRNA 3′ tail sequence composition. For COI and CYb RNAs, we observed no significant change in the nt composition of 3′ tails. In kPAP2-depleted cells, COI 3′ tails averaged 2 and 4% uridine in procyclic and bloodstream forms, respectively, while CYb averaged 23% uridine. However, in RPS12U mRNA 3′ tails, we observed a striking increase in the percentage of uridine residues, and a corresponding decrease in adenosine residues, upon kPAP2 depletion. The average uridine content of RPS12U 3′ extensions rose from 3.3% to 8.7% upon tet-induction of kPAP2 RNAi, an increase of 2.6-fold (Table 1). The sequences of RPS12U 3′ tails in uninduced and induced kPAP2 RNAi cells are presented in Table 2. We found that the increased uridine content of RPS12U 3′ tails in kPAP2-depleted cells was not manifested primarily as long uridine stretches. Rather, we observed an increased number of sites of uridine addition, at which small numbers of uridines were interspersed between adenosine stretches. The increased uridine, and thus decreased adenosine, content of RPS12U 3′ tails upon kPAP2 depletion suggests that, *in vivo*, kPAP2 contributes to the incorporation of adenosine residues in the 3′ extension of this RNA. In the absence of kPAP2, the activity of another enzyme(s) that preferentially incorporates UTP and acts in a somewhat distributive manner apparently has increased access to RPS12U 3′ ends. Because we only observed increased uridine content in one of the three RNAs examined in kPAP2-depleted cells, our results underscore the RNA specificity of 3′ tail length and composition and suggest that mitochondrial nucleotidyltransferases have differential affinity for, and/or access to, specific RNA populations.

While our examination of mRNA 3′ tail nt content suggests that kPAP2 preferentially adds adenosine residues to 3′ ends of some mitochondrial mRNAs, we could not rule out that this enzyme can also catalyze the addition of uridine residues. Therefore, we explored the possibility that kPAP2 functions as

a TUTase for ribosomal RNAs. To determine whether kPAP2 is involved in the poly(U) addition of rRNAs, we analyzed the 3′ extension of 12S rRNAs in procyclic kPAP2 RNAi cells by cRT-PCR. Upon kPAP2 down-regulation, neither the length nor the nucleotide composition on the poly(U) tail of 12S rRNA was affected (data not shown). Therefore, kPAP2 is not essential for the synthesis of poly(U) tails of rRNAs.

3.5. Analysis of mitochondrial RNA abundance and long 3′ tail synthesis in procyclic and bloodstream form kPAP2 RNAi cells

We previously showed that poly(A) tails regulate stability of mitochondrial transcripts in *T. brucei* [19,20,48]. Thus, we wanted to directly determine whether kPAP2 plays a role in regulating RNA abundance in *T. brucei* mitochondria. To this end, we analyzed the steady-state levels of several mitochondrial RNAs in uninduced and tet-induced kPAP2 RNAi cells by poisoned primer extension and northern blot. We began with procyclic form cells, using poisoned primer extension, which allows us to compare the relative abundance of edited and unedited versions of a specific transcript simultaneously. As shown in Fig. 4A, three groups of mitochondrial RNAs were examined: never-edited RNAs (COI, NADH dehydrogenase (ND) 1 and 4), RNAs whose editing is up-regulated in the procyclic stage (COII and CYb), and RNAs that are constitutively edited in both life stages (ATPase 6, ND7 5′ domain, and COIII). For all transcripts analyzed, we observed no significant difference in the abundance between the RNAs from uninduced versus induced kPAP2 RNAi cells in procyclic stage *T. brucei*.

We next used northern blot analysis to confirm poisoned primer extension results and additionally to visualize whether the polyadenylation of RNAs with long poly(A) tails (∼120–200 nt) were affected in kPAP2-depleted cells. Here, we analyzed both unedited and edited versions of CYb RNA, as well as edited RPS12 RNA from both procyclic and bloodstream form cells. Although we were unable to clearly resolve short and long tail forms of CYb mRNA in this gel, no apparent difference in size of the mRNA was detected. Similar to poisoned primer extension data, the abundance of both unedited and edited CYb RNAs remained unchanged upon kPAP2 knockdown (Fig. 4B). For edited RPS12 RNA, down-regulation of

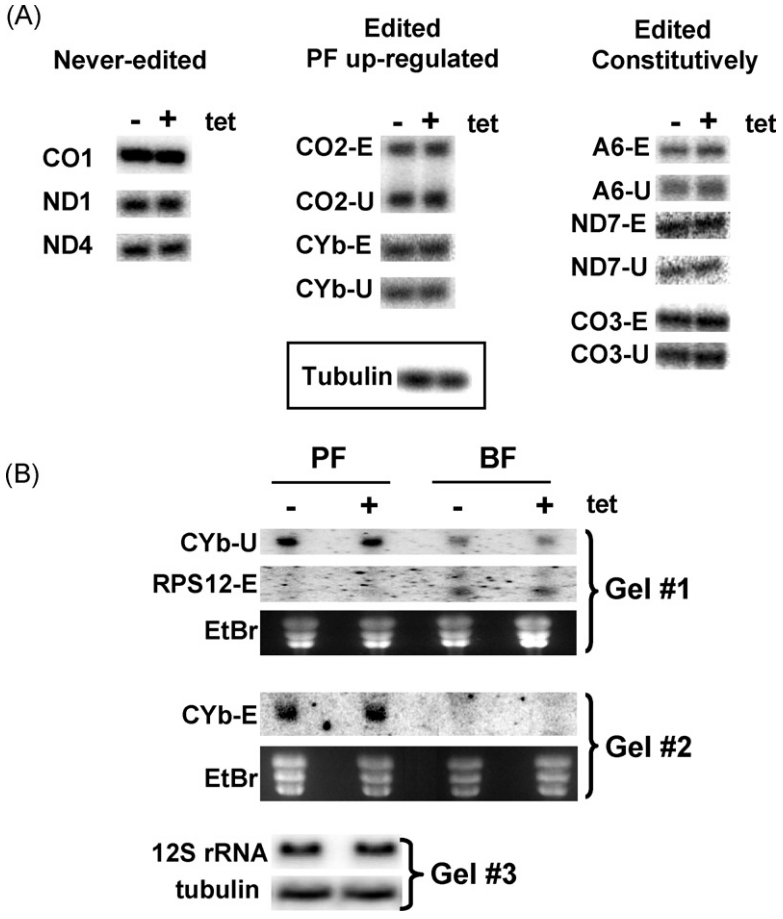

Fig. 4. Effect of kPAP2 down-regulation on the steady-state abundance of mitochondrial RNAs. (A) Twenty micrograms of RNA isolated from uninduced (−tet) and induced (+tet) procyclic form kPAP2 RNAi cells on day 4 after tet addition was subjected to poisoned primer extension analysis. Tubulin is shown as a control. (B) Twenty micrograms of RNA isolated from uninduced (−tet) and induced (+tet) procyclic (PF) and bloodstream form (BF) cells on day 4 after tet addition was subjected to northern blot analysis. Results from three individual gels are shown here. Ethidium bromide staining of ribosomal RNAs or tubulin RNA levels are shown to indicate loading. CO1: cytochrome oxidase (CO)1; ND1: NADH dehydrogenase (ND) subunit 1; ND4: ND subunit 4; CO2-E: edited CO2; CO2-U: unedited CO2, CYb: apocytochrome *b*; A6: ATPase subunit 6; ND7-E: edited ND7 5′ domain; ND7-U: unedited ND7 5′ domain; CO3-E: edited CO3; CO3-U: unedited CO3.

kPAP2 had no reproducible effect on the steady-state RPS12 RNA levels in either life cycle stage. Moreover, long poly(A) tails were present and of similar abundance in both kPAP2 induced and uninduced RNAi cells (Fig. 4B). We also examined the abundance of 12S rRNAs in procyclic form kPAP2 RNAi cells and found that the level of 12S rRNA remained unchanged upon kPAP2 depletion. The data from poisoned primer extension and northern blot analyses demonstrate that the steady-state abundance of mitochondrial transcripts, and the synthesis of long poly(A) tails, is unaffected by kPAP2 depletion.

4. Discussion

In our search for enzymes that act in mitochondrial mRNA 3′ tail synthesis in *T. brucei*, we identified a protein with high homology to the human mitochondrial PAP, which we term kPAP2. Here, we show that exogenously expressed kPAP2 is highly enriched in mitochondria, consistent with its predicted N-terminal mitochondrial import sequence. Conserved domain analysis showed that kPAP2 contains a DNA pol β-like nucleotidyltransferase motif that partially overlaps a PAP/25A domain, as well as a PAP/25A associated domain. This domain structure is conserved among members of the novel PAP family as well as putative TUTases in *T. brucei*, except for TbTUT7, which lacks the PAP/25A associated domain [32,50].

We attempted to characterize the enzymatic activity of kPAP2 *in vitro* by several approaches without success. These data were not surprising, since conserved domain analysis showed that, similar to hmtPAP and other members of the novel PAP family, kPAP2 lacks RNA-binding domains. Therefore, the presence of a bridging partner that can mediate RNA substrate-kPAP2 interaction might be required in the assay for kPAP2 to perform its enzymatic activity, resembling the model for the novel cytoplasmic PAP, GLD-2, in *C. elegans* [31]. kPAP2 associated proteins would necessarily be absent from reactions with recombinant or *in vitro* transcribed/translated enzyme. *In vivo*, binding partners may not be sufficiently abundant to associate with overexpressed myc-kPAP2. In the absence of *in vitro* catalytic activity, we cannot definitively rule out that kPAP2 functions as a TUTase or a dual PAP/TUTase. However, our *in vivo* data and the absence of a TUTase-specific insertion in the kPAP2 protein [47] strongly argue that the enzyme functions as a PAP. The future identification of kPAP2-associated proteins, potentially by tagging the protein at its endogenous locus or through yeast two-hybrid analysis, will likely be useful in the characterizing the activity of kPAP2 *in vitro*.

Targeted disruption of kPAP2 using RNAi demonstrates that this protein is not essential for growth or survival of procyclic or bloodstream form *T. brucei* cells or for bloodstream to procyclic form differentiation. These cells also exhibited no changes in the length of 3′ tails, or in the steady-state abundance of several mitochondrial RNAs examined, including never-edited and edited RNAs, or in the steady-state abundance of several mitochondrial RNAs examined. However, when we looked into the composition of 3′ tails, we detected a significant increase in the percentage of uridine residues upon kPAP2 down-regulation in RPS12U RNAs (Tables 1 and 2). The fact that kPAP2-depleted cells are still able to synthesize 3′ tails of sizes similar to those of uninduced cells, yet in different nucleotide composition, indicates the existence of other enzymes that are capable of synthesizing 3′ tails of mRNAs. However, these enzymes may display different nucleotide specificity. Several enzymes with the potential to function in this capacity have been reported. Aphasizhev [50] identified seven TUTase-related enzymes in the *T. brucei* database, of which four have been experimentally demonstrated to possess TUTase activity. Of these, KRET1 and KRET2 are mitochondrial enzymes that have a function in RNA editing [51]. Interestingly, KRET1 has also been shown to be required for UTP-dependent decay of polyadenylated RNAs in isolated *T. brucei* mitochondria by a mechanism involving RNA polymerization, suggesting it may participate in formation of mRNA 3′ ends [52]. TUT3 and TUT4 are cytoplasmic, and thus unlikely to participate in mitochondrial mRNA maturation. kPAP1 (previously termed TUT5) is a mitochondrially localized enzyme which preferentially polymerizes poly(A) *in vitro* (R. Aphasizhev, pers. comm.). Hence, kPAP1 is a strong candidate for contribution to the synthesis of mitochondrial 3′ extensions. In this report, we have renamed the previous TUT6 enzyme [32,50], kPAP2, based on its mitochondrial localization, strong homology to hmtPAP, and our *in vivo* studies demonstrating a decrease in the percentage of adenosine residues in a subset of mitochondrial RNAs in kPAP2 depleted-cells.

Based on our observations in kPAP2 RNAi cells and the knowledge of other nucleotidyltransferases, a model for the 3′ tail synthesis in *T. brucei* mitochondria can be envisioned. In this model, nucleotidyltransferases possessing specificity toward ATP or UTP, or both, participate in the polymerization of 3′ tails. kPAP2 apparently functions as a PAP, since its disruption results in decreased adenosine content in some mRNAs. In addition to kPAP2, another protein with PAP activity, potentially kPAP1, must function in this pathway, since the 3′ tails in kPAP2-depleted cells are still primarily composed of adenosine residues. The interspersed uridine residues in mitochondrial mRNA 3′ tails can be explained by the participation of a TUTase, such a KRET1. Upon kPAP2 knockdown, the activity of a TUTase(s) becomes more dominant, and this is reflected by the increased percentage of uridine residues in 3′ tails, at least in RPS12U and potentially other mitochondrial mRNAs.

The 3′ tail synthesis by these PAPs and TUTases must be strictly regulated *in vivo*, since the length and composition of 3′ tails vary among transcripts. We observed discrete mRNA-specific tail lengths for the RNAs we examined, and in the case of COI RNA, tail length was maintained throughout the life cycle. The mechanism by which specific tail lengths are dictated is unknown, and presumably involves nucleotidyltransferase-associated proteins. We also found that the 3′ tails of CYb RNAs contain a 10-fold higher percentage of uridine residues in comparison with tails of other transcripts analyzed (Table 1). These observations, together with the transcript-specific effect of kPAP2 RNAi, suggest that different combinations of nucleotidyltransferases have differential access to and/or specificity for distinct mRNAs. This regulation

may be achieved by crosstalk between transcript-specific factors and the polyadenylation/polyuridylation machineries.

In summary, our *in vivo* RNAi data suggest that kPAP2 functions as a PAP in the 3′ tail synthesis of at least some mRNAs in *T. brucei* mitochondria, although other PAPs and TUTases are apparently redundant in this pathway. To further our understanding of the machinery involved in the polyadenylation/polyuridylation of mitochondrial RNAs, it will be of interest to examine the 3′ tail composition of multiple RNAs in cells depleted for various mitochondrial nucleotidyltransferases. In addition, double (or multiple) RNAi knockdown experiments for potentially functionally redundant enzymes will also be informative with regard to the apparently complicated 3′ processing of trypanosome mitochondrial RNAs.

Acknowledgements

We thank George Cross for cell lines and anti-VSG antibodies, Fred Ponticelli for anti-myc antibodies, and Haiming Wu for advice on transfection of bloodstream form trypanosomes. These studies were supported by NIH RO1 AI47329 to LKR.

References

[1] Anderson JT. RNA turnover: unexpected consequences of being tailed. Curr Biol 2005;23(15):R635–8.
[2] Mangus DA, Evans MC, Jacobson A. Poly(A)-binding proteins: multifunctional scaffolds for the post-transcriptional control of gene expression. Genome Biol 2003;4:223.
[3] Bernstein P, Peltz SW, Ross J. The poly(A)-poly(A)-binding protein complex is a major determinant of mRNA stability in vitro. Mol Cell Biol 1989;9:659–70.
[4] Ford LP, Bagga PS, Wilusz J. The poly(A) tail inhibits the assembly of a 3′-to-5′ exonuclease in an *in vitro* RNA stability system. Mol Cell Biol 1997;17:398–406.
[5] Wilusz CJ, Gao M, Jones CL, Wilusz J, Peltz SW. Poly(A)-binding proteins regulate both mRNA deadenylation and decapping in yeast cytoplasmic extracts. RNA 2001;7:1416–24.
[6] Lisitsky I, Klaff P, Schuster G. Addition of destabilizing poly (A)-rich sequences to endonuclease cleavage sites during the degradation of chloroplast mRNA. Proc Natl Acad Sci USA 1996;93:13398–403.
[7] Carpousis AJ, Vanzo NF, Raynal LC. mRNA degradation. A tale of poly(A) and multiprotein machines. Trends Genet 1999;15:24–8.
[8] Lisitsky I, Schuster G. Preferential degradation of polyadenylated and polyuridinylated RNAs by the bacterial exoribonuclease polynucleotide phosphorylase. Eur J Biochem 1999;261:468–74.
[9] Gagliardi D, Leaver CJ. Polyadenylation accelerates the degradation of the mitochondrial mRNA associated with cytoplasmic male sterility in sunflower. EMBO J 1999;18:3757–66.
[10] Butow RA, Zhu H, Perlman P, Conrad-Webb H. The role of a conserved dodecamer sequence in yeast mitochondrial gene expression. Genome 1989;31:757–60.
[11] Tomecki R, Dmochowska A, Gewartowski K, Dziembowski A, Stepien PP. Identification of a novel human nuclear-encoded mitochondrial poly(A) polymerase. Nucl Acids Res 2004;32:6001–14.
[12] Nagaike T, Suzuki T, Katoh T, Ueda T. Human mitochondrial mRNAs are stabilized with polyadenylation regulated by mitochondria-specific poly(A) polymerase and polynucleotide phosphorylase. J Biol Chem 2005;280:19721–7.
[13] Piechota J, Tomecki R, Gewartowski K, et al. Differential stability of mitochondrial mRNA in HeLa cells. Acta Biochim Pol 2006;53:157–68.
[14] Feagin JE, Jasmer DP, Stuart K. Apocytochrome *b* and other mitochondrial DNA sequences are differentially expressed during the life cycle of *Trypanosoma brucei*. Nucl Acids Res 1985;13:4577–96.
[15] Jasmer DP, Feagin JE, Stuart K. Diverse patterns of expression of the cytochrome *c* oxidase subunit I gene and unassigned reading frames 4 and 5 during the life cycle of *Trypanosoma brucei*. Mol Cell Biol 1985;5:3041–7.
[16] Bhat GJ, Souza AE, Feagin JE, Stuart K. Transcript-specific developmental regulation of polyadenylation in *Trypanosoma brucei* mitochondria. Mol Biochem Parasitol 1992;52:231–40.
[17] Read LK, Myler PJ, Stuart K. Extensive editing of both processed and preprocessed maxicircle CR6 transcripts in *Trypanosoma brucei*. J Biol Chem 1992;267:1123–8.
[18] Souza AE, Myler PJ, Stuart K. Maxicircle CR1 transcripts of *Trypanosoma brucei* are edited and developmentally regulated and encode a putative iron-sulfur protein homologous to an NADH dehydrogenase subunit. Mol Cell Biol 1992;12:2100–7.
[19] Ryan CM, Militello KT, Read LK. Polyadenylation regulates the stability of *Trypanosoma brucei* mitochondrial RNAs. J Biol Chem 2003;278:32753–62.
[20] Kao C-Y, Read LK. Opposing effects of polyadenylation on the stability of edited and unedited RNAs in *Trypanosoma brucei* mitochondria. Mol Cell Biol 2005;25:1634–44.
[21] Read LK, Stankey KA, Fish WR, Muthiani AM, Stuart K. Developmental regulation of RNA editing and polyadenylation in four life cycle stages of *Trypanosoma congolense*. Mol Biochem Parasitol 1994;68:297–306.
[22] Decker CJ, Sollner-Webb B. RNA editing involves indiscriminate U changes throughout precisely defined editing domains. Cell 1990;61:1001–11.
[23] Koslowsky DJ, Yahampath G. Mitochondrial mRNA 3′ cleavage/polyadenylation and RNA editing in *Trypanosoma brucei* are independent events. Mol Biochem Parasitol 1997;90:81–94.
[24] Cao GJ, Sarkar N. Identification of the gene for an Escherichia coli poly(A) polymerase. Proc Natl Acad Sci USA 1992;89:10380–4.
[25] Manley JL. A complex protein assembly catalyzes polyadenylation of mRNA precursors. Curr Opin Genet Dev 1995;5:222–8.
[26] Mohanty BK, Kushner SR. Polynucleotide phosphorylase functions both as a 3′–5′ exonuclease and a poly(A) polymerase in Escherichia coli. Proc Natl Acad Sci USA 2000;97:11966–71.
[27] Yehudai-Resheff S, Hirsh M, Schuster G. Polynucleotide phosphorylase functions as both an exonuclease and a poly(A) polymerase in spinach chloroplasts. Mol Cell Biol 2001;21:5408–16.
[28] Rott R, Zipor G, Portnoy V, Liveanu V, Schuster G. RNA polyadenylation and degradation in cyanobacteria are similar to the chloroplast but different from *Escherichia coli*. J Biol Chem 2003;278:15771–7.
[29] Read RL, Martinho RG, Wang SW, Carr AM, Norbury CJ. Cytoplasmic poly(A) polymerases mediate cellular responses to S phase arrest. Proc Natl Acad Sci USA 2002;99:12079–84.
[30] Saitoh S, Chabes A, McDonald WH, et al. Cid13 is a cytoplasmic poly(A) polymerase that regulates ribonucleotide reductase mRNA. Cell 2002;109:563–73.
[31] Wang L, Eckmann CR, Kadyk LC, Wickens M, Kimble J. A regulatory cytoplasmic poly(A) polymerase in *Caenorhabditis elegans*. Nature 2002;419:312–6.
[32] Aphasizhev R, Aphasizheva I, Simpson L. Multiple terminal uridylyltransferases of trypanosomes. FEBS Lett 2004;572:15–8.
[33] Holm L, Sander C. DNA polymerase beta belongs to an ancient nucleotidyltransferase superfamily. Trends Biochem Sci 1995;20:345–7.
[34] Aravind L, Koonin EV. DNA polymerase beta-like nucleotidyltransferase superfamily: identification of three new families, classification and evolutionary history. Nucl Acids Res 1999;27:1609–18.
[35] Goulah CC, Pelletier M, Read LK. Arginine methylation regulates mitochondrial gene expression in *Trypanosoma brucei* through multiple effector proteins. RNA 2006;12:1545–55.
[36] Brun R, Schonenberger M. Cultivation and *in vitro* cloning of procyclic culture forms of *Trypanosoma brucei* in a semi-defined medium. Acta Trop 1979;36:289–92.

[37] Hirumi H, Hirumi K. Continuous cultivation of *Trypanosoma brucei* blood stream forms in a medium containing a low concentration of serum protein without feeder layers. J Parasitol 1989;75:985–9.
[38] Harris ME, Moore DR, Hajduk SL. Addition of uridines to edited RNAs in trypanosome mitochondria occurs independently of transcription. J Biol Chem 1990;265:11368–76.
[39] Wirtz E, Leal S, Ochatt C, Cross GA. A tightly regulated inducible expression system for conditional gene knock-outs and dominant-negative genetics in *Trypanosoma brucei*. Mol Biochem Parasitol 1999;99:89–101.
[40] Wickstead B, Ersfeld K, Gull K. Targeting of a tetracycline-inducible expression system to the transcriptionally silent minichromosomes of *Trypanosoma brucei*. Mol Biochem Parasitol 2002;125:211–6.
[41] LaCount DJ, Barrett B, Donelson JE. *Trypanosoma brucei* FLA1 is required for flagellum attachment and cytokinesis. J Biol Chem 2002;277:17580–8.
[42] Brun R, Schonenberger M. Stimulating effect of citrate and *cis*-aconitate on the transformation of *Trypanosoma brucei* bloodstream forms to procyclic forms in vitro. Z Parasitenkd 1981;66:17–24.
[43] Pelletier M, Read LK. RBP16 is a multifunctional gene regulatory protein involved in editing and stabilization of specific mitochondrial mRNAs in *Trypanosoma brucei*. RNA 2003;9:457–68.
[44] Kuhn J, Binder S. RT-PCR analysis of 5′ to 3′-end-ligated mRNAs identifies the extremities of cox2 transcripts in pea mitochondria. Nucleic Acids Res 2002;30:439–46.
[45] Hayman ML, Read LK. *Trypanosoma brucei* RBP16 is a mitochondrial Y-box family protein with guide RNA binding activity. J Biol Chem 1999;274:12067–74.
[46] Wang J, Bohme U, Cross GA. Structural features affecting variant surface glycoprotein expression in *Trypanosoma brucei*. Mol Biochem Parasitol 2003;128:135–45.
[47] Stagno J, Aphasizheva I, Rosengarth A, Lueck H, Aphasizhev R. UTP-bound and Apo structures of a minimal RNA uridylyltransferase. J Mol Biol 2007:882–99.
[48] Militello KT, Read LK. UTP-dependent and UTP-independent pathways of mRNA turnover in *Trypanosoma brucei* mitochondria. Mol Cell Biol 2000;20:2308–16.
[49] Militello KT, Read LK. Coordination of kRNA editing and polyadenylation in *Trypanosoma brucei* mitochondria: complete editing is not required for long poly(A) tract addition. Nucl Acids Res 1999;27:1377-85.46.
[50] Aphasizhev R. RNA uridylyltransferases. Cell Mol Life Sci 2005;62:2194–203.
[51] Stuart KD, Schnaufer A, Ernst NL, Panigrahi AK. Complex management: RNA editing in trypanosomes. Trends Biochem Sci 2005;30:97–105.
[52] Ryan CM, Read LK. UTP-dependent turnover of Trypanosoma brucei mitochondrial mRNA requires UTP polymerization and involves the RET1 TUTase. RNA 2005;11:763–73.